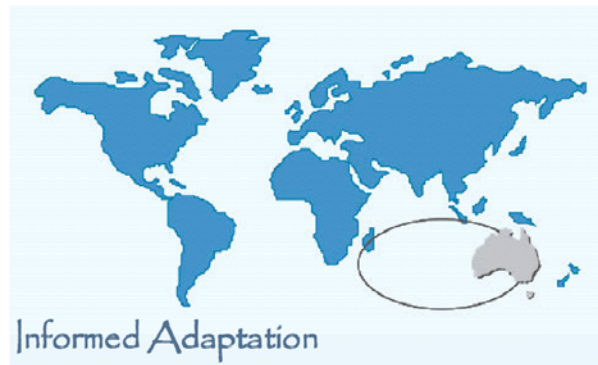# Indian Ocean Climate Initiative

Informed Adaptation

Attachment 1

Indian Ocean Climate Initiative Stage 2:

Unabridged Reports of Phase 1 Activity

July 2003 – Dec 2004

December 2004

Contents

Project 1.1: Develop methods to identify the changes in synoptic events affecting southwest rainfall – an essential first step in determining how synoptic events affecting the southwest have changed, and why.

This part of the study will develop objective techniques to determine the number and intensity of various synoptic events using historical synoptic analyses and synoptic observations, and will relate them to southwest rainfall and other climate variables to determine the relative importance of the various events in the region.

Contributors: Pandora Hope, Neville Nicholls, Lynda Chambers
Acknowledgments: Wasyl Drosdowsky, Bertrand Timbal

1.1.1   Synoptic Classification – Self-Organising Map

A computer-assisted technique has been used to cluster synoptic maps of mean sea-level pressure into a limited number of types, a 'Self-Organising Map' (SOM). The method has been used previously to analyse the frequency of synoptic systems (e.g. Hewitson & Crane 2002), to determine the synoptic situations associated with high wind events (Cassano et al. 2004) and as part of a downscaling method to explore the drivers of extreme precipitation (Cavazos 1999, 2000). A SOM has been used here to cluster synoptic maps into types and to assess how the frequency of each type changes through time. A composite of rainfall on days corresponding to each synoptic type is also produced.

Both NCEP/NCAR (1948-2003) and ERA40 (1958-2001) reanalyses for June and July mean sea-level pressure were used to develop a SOM. In general, the synoptic types in the SOM produced with each of the two reanalyses data sets are similar. The numerical model used for creating the ERA40 data is a more recent model run at higher resolution than that used for the NCEP/NCAR reanalysis, and for many features since 1979 the results are closer to actual measurements. Unfortunately, over the southwest, the sea-level pressure from ERA40 does not follow the data as closely as the NCEP/NCAR reanalysis prior to 1976. Since about 1976, ERA40 and NCEP/NCAR mean sea-level pressure values over the southwest are very close. The NCEP/NCAR reanalysis was chosen for further analysis.

There are a number of options when developing a SOM, including the number of clusters (types), and the size of the spatial domain of the data. Using the entire Australian domain allows pressure variations in the east to modify the clustering process. A domain ranging from 90 to 130°E and 15 to 50°S was found to capture the variability associated with systems affecting rainfall in the southwest. Two SOMs were produced and assessed, one of 20 synoptic types, and one of 35 types. Both SOMs showed wet types decreasing in frequency since the mid 1970s while the dry types increased in frequency. The larger (35 type) SOM reveals some structures not evident in the smaller SOM, for example, a region of low pressure extending south from the tropics, possibly linked with northwest cloud-bands. From the SOM of 20 types, Figure 1.1 shows the sea-level pressure pattern of a synoptic type linked with wet conditions (type 17) and one linked with dry conditions (type 2). The rainfall anomaly linked with these types is shown in Figure 1.2.

Rainfall in the southwest is also known to be linked with upper level features, and the rainfall anomaly matching each synoptic type when data from higher levels is included in the development of the SOM is clearer. Further analysis of this SOM, shifts in the amount of rainfall associated with each synoptic type and the link between the synoptic types and features such as northwest cloud-bands will be examined in further work.
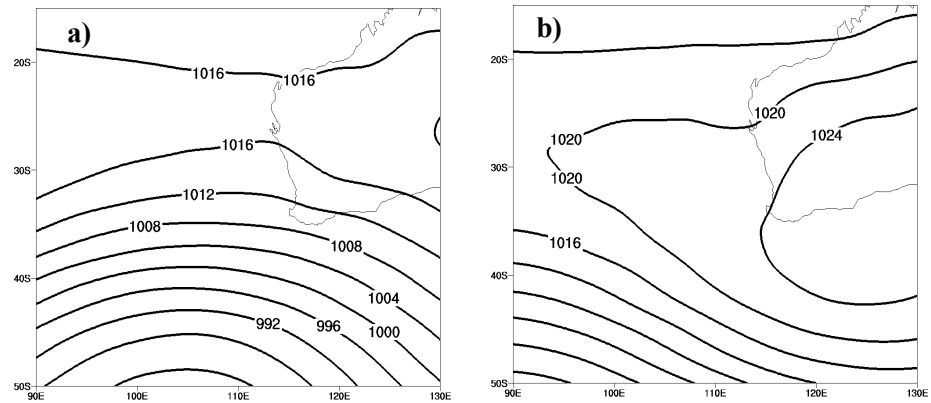
Figure 1.1 NCEP 0Z & 12Z sea level pressure SOM of 20 types:
a) Type 17
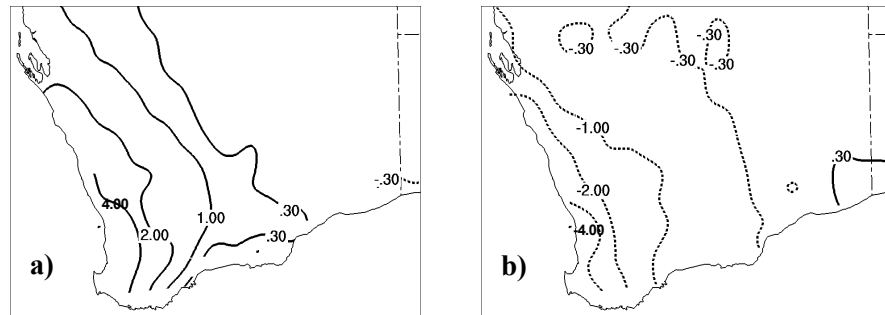**b) Type 2**

Figure 1.2. Rainfall anomaly (mm/day) associated with SOM type:
a) 17
 b) 2

1.1.2   Shifts in Perth rainfall moisture source

Shifts through time in the preferred path of air trajectories leading to high rainfall events at Perth Airport highlight shifts in the source region of moisture. Such shifts may also help identify the frequency of particular types of synoptic systems associated with rain events, for example northwest cloud-bands. Three-dimensional backward trajectories were started at various heights above Perth and traced back through NCEP/NCAR reanalysis data using HYSPLIT. Trajectories along 500 and 800 hPa pressure surfaces were also traced using interpolation methods in ERA40 reanalysis data. Two-dimensional trajectory density maps were created by counting the number of trajectories in 1°×1° boxes. The patterns of trajectory density are surprisingly similar using both datasets. The trajectory paths are highly sensitive to the time at which they are started. Large winter rainfall totals in the southwest are generally associated with the pre-frontal air-mass, and thus it is important to capture the timing of the front accurately. Starting from model rainfall events rather than actual rainfall more accurately captured this timing, particularly prior to 1975. The weighted difference between the trajectory density maps for 1948-1975 and 1976-2003 (Figure 1.3) show that the preferred moisture source and direction of approach is from further south in the later period. The features driving these shifts need further consideration and analysis.
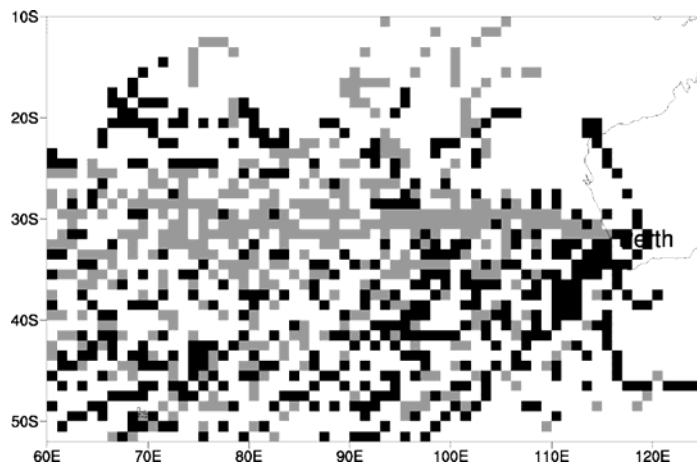
Figure 1.3. Relative frequency of air parcel trajectories back from high rain events at Perth Airport. Regions where there were more trajectories in 1976-2003 are in black; where there were more in 1958-1975, in grey. The white areas are where there were fewer than 4 trajectories in either period.

1.1.3 Large-scale features and their changes

Cyclone statistics from a surface cyclone tracking scheme and their changes have been discussed in the literature (e.g. Simmonds & Keay 2000, IOCI 2002). Cyclone depth is known to correlate well with rainfall. The correlation between winter rainfall over the southwest and cyclone depth was calculated, and found to change sign between the early (1958-68) and late (1976-97) periods, although the shift was not statistically significant.

1.1.4 Analysis of station data - shifts in rain bearing storms reflected at the surface

The direction of station winds during rain-days at Wandering, Perth Airport and Cape Leeuwin was assessed, following a similar method to Wright (1974). At Wandering and Perth Airport the wind is mostly from the north during rain-days in June and July and the rainfall when the wind is from the north far exceeds the rainfall totals when the wind is from any other direction (Figure 1.4). Rainfall associated with winds from the north and northeast has decreased since the 1970s at Wandering and Perth Airport. At Perth Airport (Figure 1.4) the average monthly rainfall associated with winds from the east (predominantly from the northeast) was markedly lower during the two later epochs than in 1944-1959. This indicates that synoptic systems associated with surface winds from the northeast have contributed to the rainfall decline.
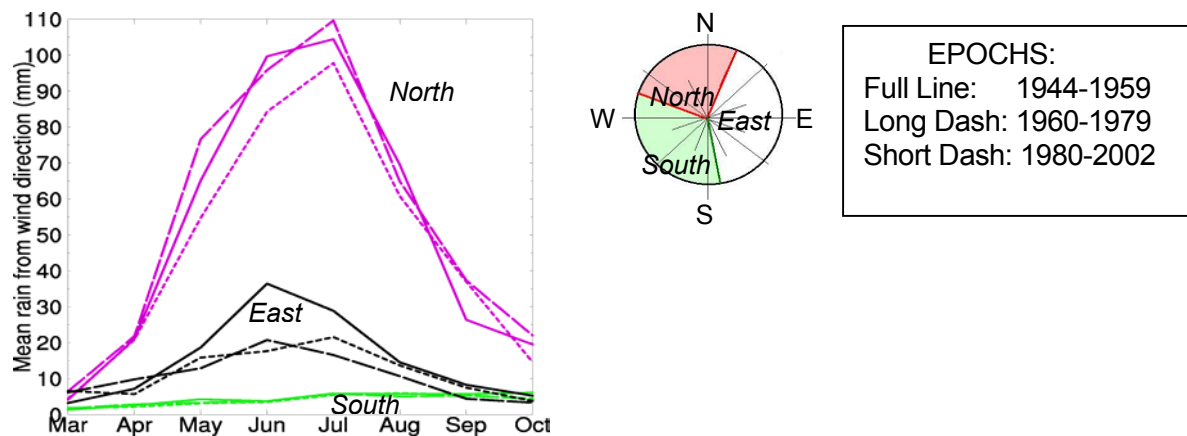
5

Figure 1.4. Perth Airport average monthly rainfall amounts associated with winds from directions as shown by the shaded segments on the compass above. There is more rainfall linked with winds from the north in all epochs.

1.1.5 Methods examined and discarded

1. Analysis of the principal modes of variance in mean sea level pressure (described by Drosdowsky 1993) was carried out however, the physical meaning of the results was difficult to interpret.

2. A clustering technique ('tree') resulted in one or two very large clusters plus many smaller ones, without capturing all the expected synoptic types.

References

Cassano, E.N., A. H. Lynch and M.R. Koslow, 2004: Classification of synoptic patterns in the western Arctic associated with high wind events at Barrow, Alaska. *submitted to: Geophysical Research Letters.*

Cavazos, T, 1999: Large-scale circulation anomalies conducive to extreme precipitation events and derivation of daily rainfall in northeastern Mexico and southeastern Texas. *Journal of Climate*, **12**, 1506-1523.

Cavazos, T, 2000: Using Self-Organizing Maps to investigate extreme climate events: An application to wintertime precipitation in the Balkans. *Journal of Climate*, **13**, 1718-1732.

Drosdowsky, W, 1993: An analysis of Australian seasonal rainfall anomalies: 1950-1987. I: Spatial patterns. *International Journal of Climatology*, **13**, 1-30.

Hewitson, B. C. and R.G. Crane, 2002: Self-organizing maps: Applications to synoptic climatology. *Climate Research*, **22**, 13-26.

IOCI, 2002: Climate variability and change in south west Western Australia. Indian Ocean Climate Initiative Panel, 34pp.

Simmonds, I. and K. Keay, 2000: Variability of Southern Hemisphere extratropical cyclone behavior. *Journal of Climate*, **13**, 1958-97.

Wright, P.B., 1974: Seasonal rainfall in southwestern Australia and the general circulation. *Monthly Weather Review*, **102**, 219-232.

Project 1.2: Determine the mid-1970s changes in the Southern Hemisphere circulation.

This project will examine the mean circulation before and after the mid-1970s decrease in rainfall in the southwest. These will be compared with different model circulations associated with anthropogenic climate change due to increasing greenhouse gases and other composition changes associated with human activity.

Contributors: Carsten S. Frederiksen (BMRC) and Jorgen S. Frederiksen (CAR)

1.2.1 Analysis of NCEP reanalysis data for the Southern Hemisphere winter

The global Southern Hemisphere (SH) winter climates for the periods 1949-1968 and 1975-1994, using the NCEP/NCAR reanalysis (Kalnay et al., 1996), have been compared and there are significant differences between the two periods. Most noticeable is a reduction of 20% in the peak strength of the SH subtropical jet stream. Figure 1.5 shows the height (in pressure units) and latitudinal cross-section of the SH zonal (east-west) wind, averaged over 100˚E-130˚E longitude.
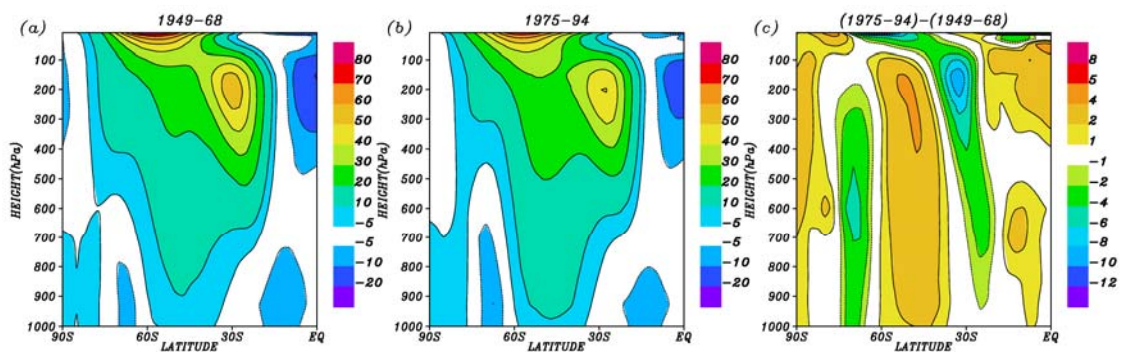

Figure 1.5. Vertical cross-section of the Southern Hemisphere July zonal wind (ms⁻¹) averaged over 100˚E-130˚E longitude for the periods (a) 1949-1968, (b) 1975-1994 and (c) their difference.

In both periods, there is a maximum in the zonal wind strength in the subtropics (near 30˚S) at about the 200 hPa pressure level. In the later period, there is a reduction of about 10 ms⁻¹ in this maximum. This is directly associated with changes in the Hadley (north-south) circulation in the Southern Hemisphere. There have also been substantial changes in the Walker (east-west) circulation with increased upper level wind divergence in the eastern tropical Pacific in the latter period.

The thermal structure of the SH atmosphere has also changed with a significant warming south of 30˚S, tending to reduce the equator-pole temperature gradient (Figure 1.6).
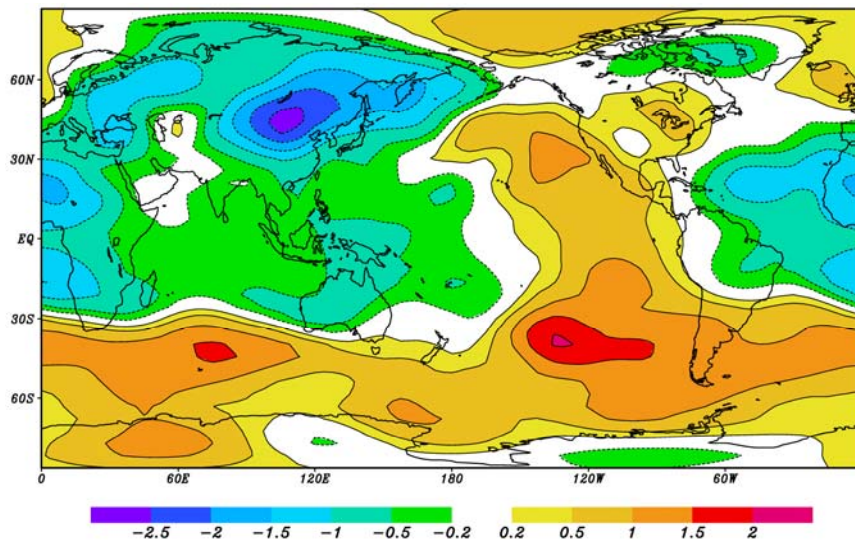
Figure 1.6 Difference in the vertically averaged July temperature (K) for (1975-1994) - (1949-1968).

Such changes would be expected to have a significant effect on the stability of the SH circulation and hence on the likelihood of SH large-scale weather system development, which might have a major impact on southwest Western Australia.

An analysis, of the impact of these observed SH winter climate changes on the nature of the dominant SH weather modes (preferred atmospheric states), was conducted. Particular emphasis was placed on the storm track modes, that are associated with the storms that affect southwest Western Australia. Here, we have used the primitive equation instability model described in Frederiksen and Frederiksen (1992, 1993a, 1993b, and 1997) to identify the dominant unstable weather modes in each period. In the earlier period, the dominant weather mode is a mode which affects southern Australia, and has largest impact over southwest Western Australia (Figure 1.7a and Figure 1.8a). This mode consists of a series of eastward propagating troughs (blue shading) and ridges (red shading), and is shown in Figure 1.7a at a particular phase (or instant). As the troughs and ridges move eastward they amplify to reach a maximum in preferred regions.
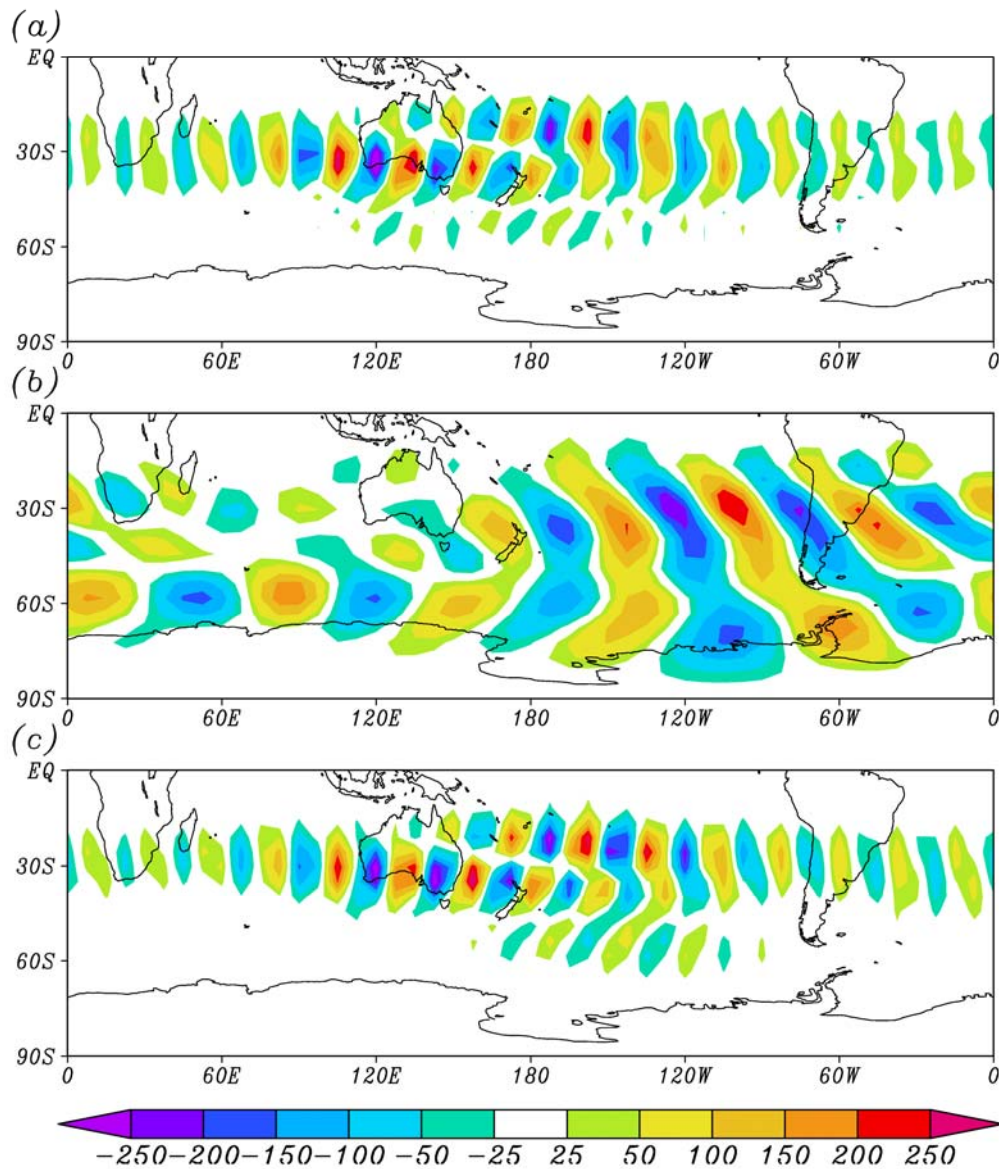
Figure 1.7. The dominant weather modes for July, for the periods (a) 1949-1968 and (b) 1975-1994. Shown are the upper level troughs (blue) and ridges (red) at a particular phase (instant). The second most important July weather mode, for the period 1975-1994, is shown in (c). Arbitrary units .

Figure 1.8a shows the storm track associated with the dominant mode in the early period and indicates that its largest impact (red shading) is over south-western Australia. By contrast, in the latter period, the dominant SH mode has a different horizontal structure (Figure 1.7b). In particular, this weather mode effectively bypasses southwest Western Australia and has maximum impact in the central south Pacific. There is, however, a subdominant weather mode (Figure 1.7c), with a similar structure to the dominant mode from the earlier period, however its largest impact has shifted to be over eastern Australia (Figure 1.8b), and the mode's growth rate is reduced by more than 30%. Other weather modes are also less likely to grow in the later period. The changes in the SH winter climate since the mid-1970s have led to a reduction in the likelihood of the development of the large-scale weather systems that affect southwest Western Australia.
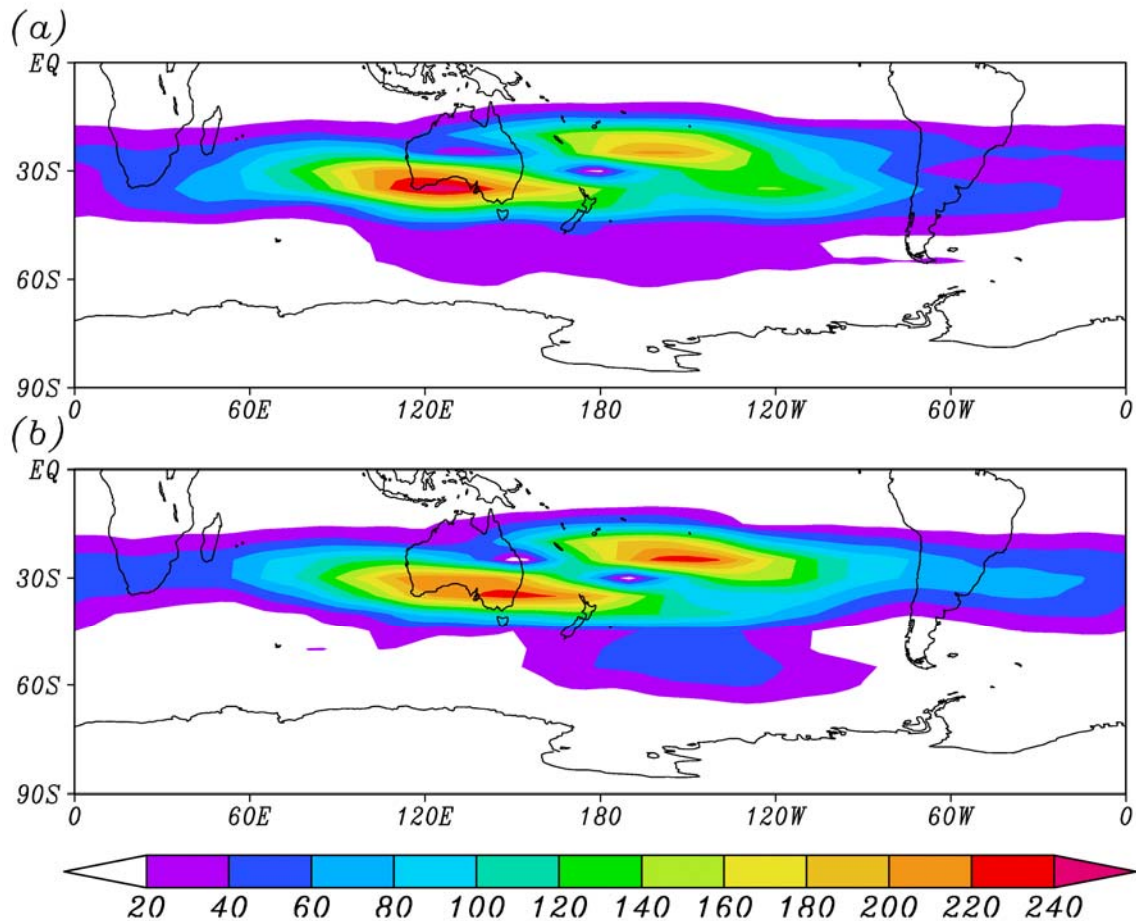
Figure 1.8. The upper level storm tracks associated with the dominant July weather modes in Figures 7a and 7c. Shown here is the relative impact (shaded) of the weather systems as they develop and propagate eastward.

It is clear from this initial study that there has been a shift in the storm track and a reduced potential for the development of weather systems in the SH between the two periods. We still have to evaluate the effects of the observed changes in the SH climate on other modes of variability that also affect Australian rainfall (e.g. Northwest Cloudband modes, the Southern Annular Mode, and other teleconnections). But, we suspect that the changes in the nature of the storm track modes are probably the most important.

While the observed changes in the SH climate are not inconsistent with climate change due to anthropogenic forcing from increasing greenhouse gases, this has still to be established. In future studies, similar analyses of coupled model simulations will try to establish the effects of increasing greenhouse gases, sulphate aerosols and trends in ozone depletion, both singly and in combination, on the SH climate and the storm tracks (and other modes of weather variability) to see if the observed changes can be attributed to such climate forcings.

References

Frederiksen, C.S. and J.S. Frederiksen, 1992: Northern Hemisphere Storm Tracks and Teleconnection Patterns in Primitive Equation and Quasigeostrophic Models. *Journal of the Atmospheric Sciences*, **49**, 1443-1458.

Frederiksen, J.S. and C.S. Frederiksen, 1993(a): Monsoon disturbances, intraseasonal oscillations, teleconnection patterns, blocking and storm tracks of the global atmosphere during 1979 : Linear theory. *Journal of the Atmospheric Sciences*, **50**, 1349-1372.

Frederiksen, J.S. and C.S. Frederiksen, 1993(b): Southern Hemisphere storm tracks, blocking and low-frequency anomalies in a primitive equation model. *Journal of the Atmospheric Sciences*, **50**, 3148-3163.

Frederiksen, J.S. and C.S. Frederiksen, 1997: Mechanisms of the Formation of Intraseasonal Oscillations and Australian Monsoon Disturbances: The Roles of Convection, Barotropic and Baroclinic Instability. *Beitrage zur Physik Atmosphare*, **70**, 39-46.

Kalnay, E., M. Kanamitsu, R. Kistler, W. Collins, D. Deaven, L. Gandin, M. Iredell, S. Saha, G. White, J. Woollen, Y. Zhu, M. Chelliah, W. Ebisuzaki, W. Higgins, J. Janowiak, K. C. Mo, C. Ropelewski, J. Wang, A. Leetmaa, R. Reynolds, R. Jenne, and D. Joseph, 1996: The NMC/NCAR 40-Year Reanalysis Project. *Bulletin of the American Meteorological Society*, **77**, 437-471.

Project 1.3:   The role of multi-decadal variability will be assessed by analyzing the results from a CSIRO Mark3 climate model run for several hundred years under present-day conditions

This component of the project aims to identify drivers of multi-decadal variability which are independent of greenhouse forcing. The CSIRO Mark3 climate model has been used to provide an unforced simulation of present-day climate, which represents a "control" simulation against which other climate experiments can be compared.

Contributors: Wenju Cai, Brian Ryan, Ge Shi and Mark Collier
Acknowledgement: Siobhan O'Farrell, Paul Durack

The climatological winter rainfall over the southwest from the CSIRO Mark 3 coupled model, covering a multi-century (500 year) period run under "control" conditions, shows significant decadal and inter-decadal fluctuations. Figure 1.9 displays a time series of the winter season (June, July and August; JJA) rainfall anomaly over a 500-year period, expressed as a percentage of the climatological winter mean. Superimposed is a 13-year running mean. The model winter rainfall running mean shows several multi-decadal-long drying trends at a rate of 20-30% over a period of 20-30 years. Further, it indicates that a drying trend can last for up to 70 years. Thus, the amplitude of winter rainfall decrease resulting from multi-decadal variability could be comparable to what has been observed since the late 1960s.
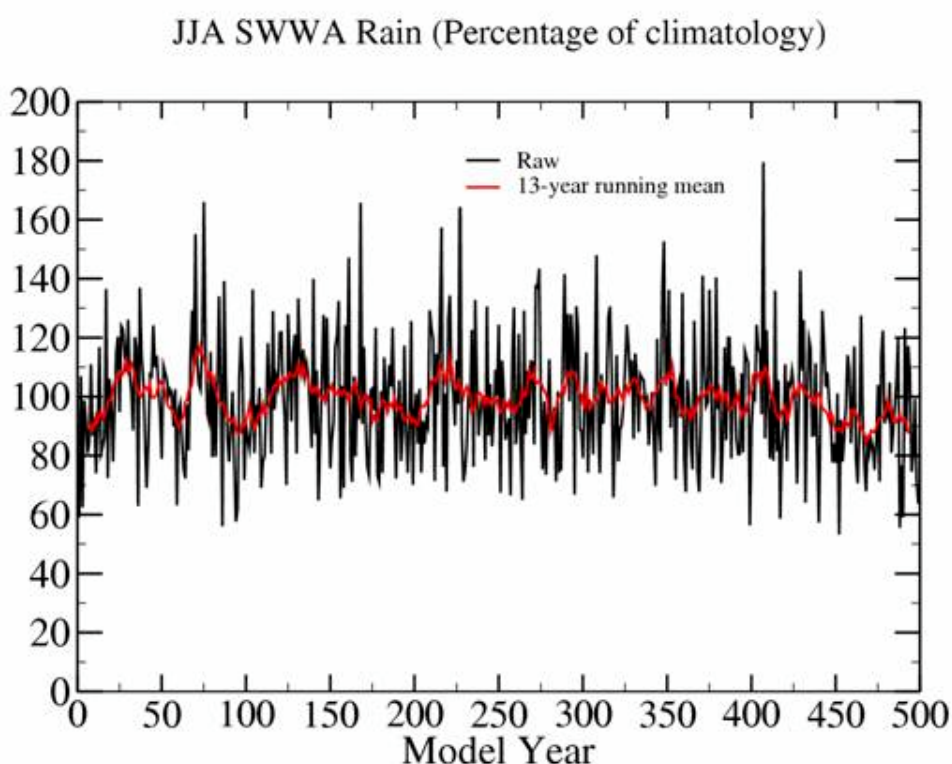

Figure 1.9 Time series of model winter rainfall over southwest Western Australia as a percentage of the climatological average. A 13-point running mean version is superimposed.

To explore potential causes for the multi-decadal rainfall variability, and its possible linkage with variability of mean sea level pressure, we applied empirical orthogonal function (EOF) analysis to sea-level pressure anomalies. The first EOF (Figure 1.10a) accounts for about 61% of the total variance, with the variance of the second EOF (Figure 1.10b) dropping to 8% of the total variance.

The first EOF is the southern annular mode (SAM), which displays out-of-phase mid- and high-latitude variations. The time-series associated with the first EOF (SAM) has higher values corresponding to the pattern in Figure 2a, with high pressure across southern Australian latitudes and low pressure further south, while lower values in the time-series correspond to lower pressures across Australian latitudes. The 13-year running mean of the time series associated with the SAM (normalised) is plotted in Figure 2c (black curve) together with the 13-year running mean for winter southwest Western Australia rainfall (red curve). The rainfall fluctuations have corresponding signals in the SAM, with a decrease in rainfall associated with anomalously higher sub-tropical sea-level pressure (high mode of the SAM).
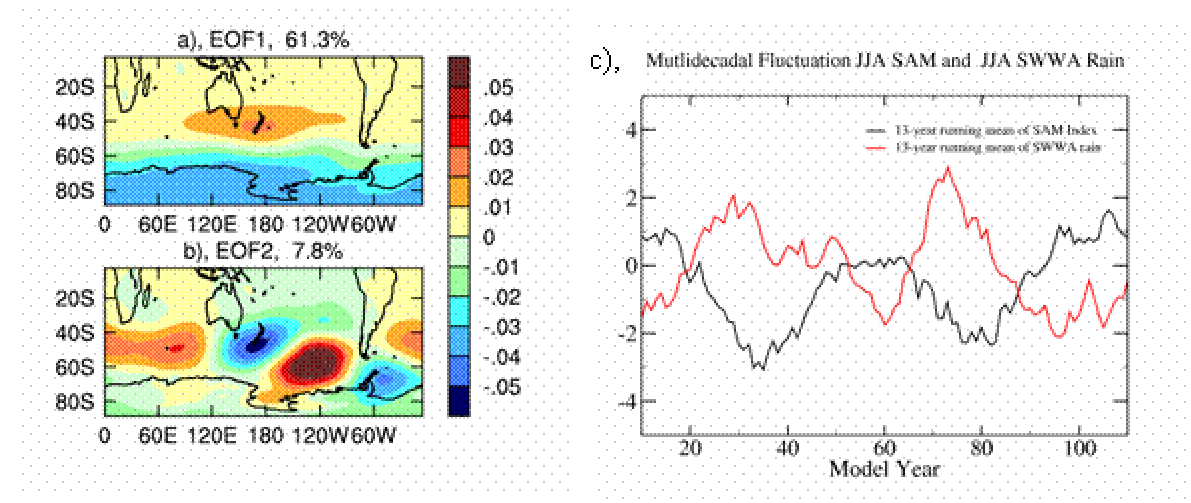

Figure 1.10. Dominant variability patterns of MSLP from EOF analysis. The first mode (panel a) is the SAM and accounts for 61% of the total variance, the second mode is shown in panel b, and only explains 8% of the variance. The 13-point running mean of the winter time series is associated with the first mode and is shown in panel c, along with a 18-point running mean of winter rainfall.

The global context of the climate anomalies linked to SAM is examined in Figure 1.11, which depicts maps of the correlation between the time series of the SAM and grid-point rainfall (Figure 1.11a), sea-level pressure (Figure 1.11b), zonal (east-west) wind (Figure1.113c) and sea-surface temperature (Figure 1.11d). The rainfall change over the southwest Western Australia region is part of large scale anomalies associated with the increasing mid-latitude sea-level pressure and decreasing mid-latitude westerlies. Over the high latitudes, sea-surface temperature is anomalously low, due to enhanced cloud cover attributed to the decreasing sea-level pressure. It is obvious that the most important mode of variability in the sea-level pressure (SAM) is closely linked to many aspects of the global climate, including southwest Australian rainfall.
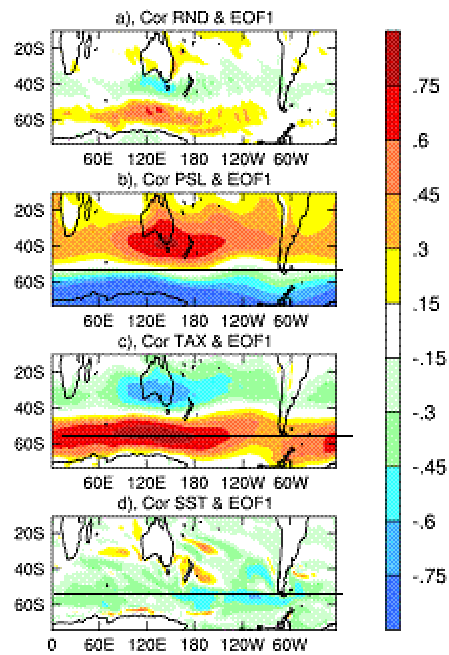
13

Figure 1.11. Maps of correlation coefficients between the SAM index and (a) rainfall, (b) sea-level pressure, (c) zonal (east-west, to the east is positive) wind, and d) sea-surface temperature.

The generation of multi-decadal variations of the SAM is not yet well understood. Previous studies (Watterson 2000; Cai and Watterson 2002) found that in models without oceanic feedback the SAM has variations on multi-decadal time scales, indicating that the atmosphere alone can drive multi-decadal variability. The model analysed here has an atmosphere coupled to an ocean, and the multi-decadal component of the variability is more pronounced, thus it is of interest to examine the possible role of the oceanic circulation in driving multi-decadal variability with this model. The mean overturning circulation, which is the mean vertical and meridional (north-south) movement, (Figure 1.12a) shows the Antarctic Bottom Water Formation, the Deacon cell, in red, centred at about 50˚S, and the North Atlantic Deep Water Formation cell. Fig 1.12b shows the correlation between the overturning and the time-series of SAM. North and south of the Deacon cell, strong anomalies (which penetrate to a depth of more than 2000 m) are generated by wind anomalies associated with the SAM. The setup of the overturning circulation anomalies is such that the sea-surface temperature anomalies are reinforced, which may contribute to the multi-decadal time scale.

Attributing the rainfall decline to a specific cause is not a trivial task. Multi-decadal variability is seen in models with no anthropogenic forcing, possibly enhanced by feed-backs with the ocean, however anthropogenic forcing also contributes to persistent climate states. Most climate models with climate change forcing simulate an increase in mid-latitude mean sea level pressure in response to increased atmospheric CO_2. This increase is expressed as a shift to higher values of the southern annular mode (SAM), with higher pressures in the Australian region. Earlier studies have shown that rainfall over south west western Australia, a region affected by the increasing pressure, decreases as CO_2 increases (Cai et al., 2003). Ozone depletion can also generate an upward trend in the SAM (Sexton, 2001).
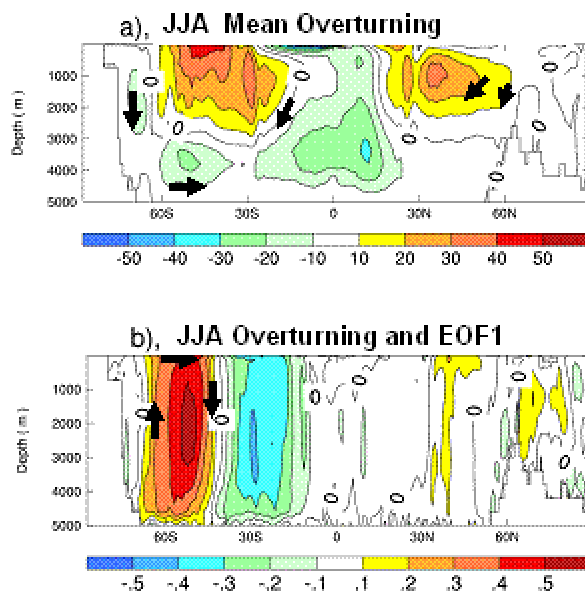
14

Figure 1.12. Model oceanic overturning circulation for winter season (a), and anomaly pattern associated with the SAM (b). Oceanic overturning is the mean vertical and meridional (north-south) motion. In (a), Antarctic Bottom Water Formation follows the arrows at the left, the Deacon Cell is the circulation in red centred at 50˚S, and North Atlantic Deep Water Formation follows the arrows in the Northern Hemisphere.

Thus the result from this component of the project suggests that either or both climate change forcing and natural multi-decadal variability could have generated the observed drying trend in the southwest. However, in a further experiment forced with observed and projected climate changes, winter rainfall drops below the range of natural variations (Figure 1.13), reinforcing the concept that climate change will play a more prominent role in the winter rainfall decrease over the southwest.
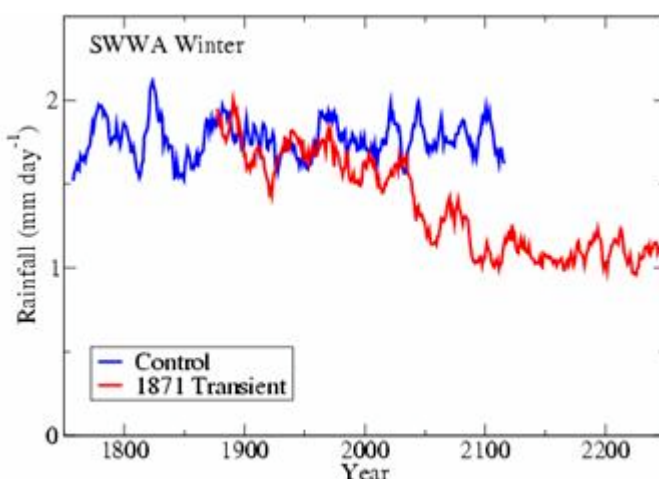

Figure 1.13. Model winter rainfall over southwest Western Australia from control simulation (blue) and climate change simulation (red curve) of the CSIRO Mark 3 model.

References

Cai, W. J., Whetton, P. H., and Karoly, D. J (2003): The response of the Antarctic Oscillation to increasing and stabilized atmospheric CO2. *Journal of Climate*, **16**, 1525-1538.

AABW

15

Cai, W. J., and Watterson, I. G. (2002): Modes of interannual variability of the Southern Hemisphere circulation simulated by the CSIRO climate model. *Journal of Climate*, **15**, 1159-1174.

Sexton, D. M. H., (2001): The effort of stratospheric ozone depletion on the phase of the Antarctic Oscillation. *Geophysical Research Letters*, **28**, 3697-3700.

Watterson, I. G., (2000): Southern mid-latitude zonal vacillation and its interaction with the ocean in GCM simulations. *Journal of Climate*, **13**, 562-578.

Reanalysis datasets and potential problems

Contributor: Pandora Hope

What are the reanalysis datasets?

Many meteorological institutions run numerical models of the atmosphere after assimilating current observations to create forecasts for hours and days into the future. The result is gridded datasets for many atmospheric variables, enhancing the availability of 'data' beyond what is available solely from observations. These datasets became a valuable resource for climate studies; however, changes in the models as they develop led to inconsistencies in the analysis over time. Groups in the United States of America and Europe decided to 'fix' their model and analysis system at the most recent version, and re-assimilate the observations (and some new ones) through time to create a continuous data-set which could be used for studies of the weather and climate. Hence the name 'reanalysis'.

There are four major reanalysis datasets, ERA15, ERA40, NCEP/NCAR reanalysis and NCEP-DOE Reanalysis 2. The European Centre for Medium-range Weather Forecasts (ECMWF) produced ERA15 and ERA40. ERA15 was run for 15 years from December 1978 to February 1994. ERA40 is a more recent product, and gridded daily data are now available on the web. ERA40 was run from September 1957 to August 2002. The U.S. has also produced two reanalysis sets that are available over the internet. The first was the National Center for Environmental Protection / National Center for Atmospheric Research (NCEP/NCAR) reanalysis. This is still extensively used as it was started from the earliest date – January 1948 and is updated continuously. The second was run at the Department Of Energy (DOE), and is thus called the NCEP-DOE Reanalysis 2. This second reanalysis corrected some of the problems evident in the NCEP/NCAR reanalysis, but it does not extend back for as many years (yet) and the processing tools available on the internet are not as extensive, so it is used less at this stage. Access to the data is often from the site of the institution that ran the project or related sites, but there are some sites that are available to manipulate the data in useful ways, eg.,: http://climexp.knmi.nl/, http://www.cdc.noaa.gov/map/

High/low quality fields

Kalnay et al. (1996) classify the output fields of the NCEP/NCAR reanalysis into four quality categories; these depend on the relative influence of the observational data or model on the output field. These categories will apply to most other reanalyses available at present. The first category includes fields that are strongly influenced by observational data (sea-level pressure, upper air temperature and winds), while the model has a stronger influence on fields in the second category, for example humidity and surface temperature (ERA40 directly assimilates surface temperatures after 1967, so this would likely be in the first category). Fields derived solely from the model fall into the third category (precipitation and surface fluxes). The fourth category is for fields that are only climatological, such as the land-sea mask. For a full list of the suggested quality of fields, refer to Kalnay et al. (1996).

ERA40

Description of Model used

Excerpt from ERA40 Project Report Series No. 8: "The ECMWF forecast system is called the Integrated Forecasting System (IFS) and has been developed in co-operation with Meteo-France. For ERA40 it is used with 60 levels, from the top of the model at 0.1 hPa to the lowest model level at about 10 m above the surface. The spectral resolution is TL-159 (triangular truncation at wave number 159) with a corresponding resolution of about 125 km in grid point space. In grid point space, a so-called Reduced Gaussian grid is used which has 320 points around the world at the equator, but the number reduces at higher latitudes to obtain a nearly constant grid spacing at all latitudes."

Assimilation

Excerpt from ERA40 Project Report Series No. 8: "The analysis uses the so-called 3-dimensional variational method (3DVAR+FGAT), where a cost function in relation to observations and background is minimized. The weighting of the different parts of the cost function is controlled by

estimates of observation errors and background errors. ... Most satellite observations (e.g. from TOVS instruments) are used by computing radiances from the model fields (forward model) and by comparing them with the satellite radiances. The analysis system uses a wide range of observations, from conventional radiosonde and SYNOP observations, to ocean winds from satellite scatterometry."

Data availability

The model output data has been interpolated to a 2.5°×2.5° grid and is available on the web at:
http://www.ecmwf.int/research/era/
http://data.ecmwf.int/data/d/era40_daily/
(ERA15: http://www.ecmwf.int/research/era/ERA-15/)

Performance

http://www.ecmwf.int/research/era/Performance/index.html
In the ERA40 Project Report Series No.18 (Simmons 2004), the dataset of surface temperature, CRU, was compared with reanalysis output. It is pointed out that "...there were few surface observations available for assimilation in ERA40 prior to 1967...", and this leads to "...a pronounced (and almost certainly erroneous) cooling over much of Australia." NCEP/NCAR does not assimilate surface temperature measurements at all, but calculates temperature from the radiation balance, but the report found that "...NCEP/NCAR is closer than ERA40 to CRU full-period trends for Australia...". Ian Watterson (CSIRO) has done a preliminary analysis of trends and variations in the ERA40 data and found that: "The precipitation over tropical oceans increased dramatically after 1991, when satellite-based humidity data were incorporated into the reanalysis." Watterson (2004) also notes a jump in tropical precipitation in 1973. There is an artificial increasing trend in kinetic energy, particularly in the extra-tropics of the Southern Hemisphere (Bengtsson, 2004).

Documentation

http://www.ecmwf.int/publications/library/do/references/list/192

Watterson, I.G., 2004: A preliminary assessment of trends and variations in ERA40 Reanalysis Data, including comparisons with NCEP-R1, for the broad Australian Region. CSIRO

Simmons, A.J., P.D. Jones, V. da Costa Bechtold, A.C.M. Beljaars, P.W. Kållberg, S. Saarinen, S.M. Uppala, P. Viterbo and N. Wedi, 2004: Comparison of trends and variability in CRU, ERA40 and NCEP/NCAR analyses of monthly-mean surface air temperature. submitted to *Journal of Geophysical Research - Atmospheres*

Bengtsson, L., S. Hagemann and K.I. Hodges, 2004: Can climate trends be calculated from reanalysis data? *Journal of Geophysical Research*, **109**, D11111

NCEP/NCAR

Description of Model used

The model used to produce the NCEP/NCAR reanalysis is a spectral model run at T62 with 28 levels in the vertical. The horizontal resolution is approximately 1.9° longitude by 1.9° latitude.

Data assimilated

The data that were prepared for assimilation includes synoptic data from surface stations, soundings from the surface and satellite, aircraft data and winds from a microwave imager. Ocean data are from ships, buoys and research vessels.

Data availability

Flux data are available on a grid of ~1.9°×1.9°, while other fields are available on a 2.5°×2.5° grid.
http://www.cdc.noaa.gov/cdc/reanalysis/

Performance

http://www.cdc.noaa.gov/cdc/reanalysis/problems.shtml
Problems have been identified while the reanalysis was being produced, and many of those problems have been corrected and the affected time periods re-run, and the data now available on the web are not affected by those problems. Some problems that may have a large effect on the southwest of Western Australia and are still present in the reanalysis include: 2 m and skin temperatures over land are often too hot when winds are less than 0.75 m/s; Estimates of sea-level pressure for the Southern

Ocean were shifted by 180 degrees longitude for the years 1979-1992 before being assimilated into the model. This has a reasonable influence on smaller time and space scales south of 40˚S.

Documentation
http://www.atmos.umd.edu/~ekalnay/Kistleretal.pdf
Kalnay, E., M. Kanamitsu, R. Kistler, W. Collins, D. Deaven, L. Gandin, M. Iredell, S. Saha, G. White, J. Woollen, Y. Zhu, M. Chelliah, W. Ebisuzaki, W. Higgins, J. Janowiak, K. C. Mo, C. Ropelewski, J. Wang, A. Leetmaa, R. Reynolds, R. Jenne, and D. Joseph, 1996: The NMC/NCAR 40-Year Reanalysis Project. *Bulletin of the American Meteorological Society*, **77**, 437-471

NCEP/DOE Reanalysis-2
Data source
http://wesley.wwb.noaa.gov/reanalysis2
Documentation
Kanamitsu, M., W. Ebisuzaki, J. Woolen, J. Potter, and M. Fiorino, 2000: Overview of NCEP/DOE Reanalysis-2. In: Proceedings of the second World Climate Research Programme (WCRP) international conference on reanalyses, 1999. 1-4

Mean results in the southwest
Resolution
The resolution of a 2.5°×2.5° grid is relatively coarse when considering a region the size of the southwest (Figure 1.14).
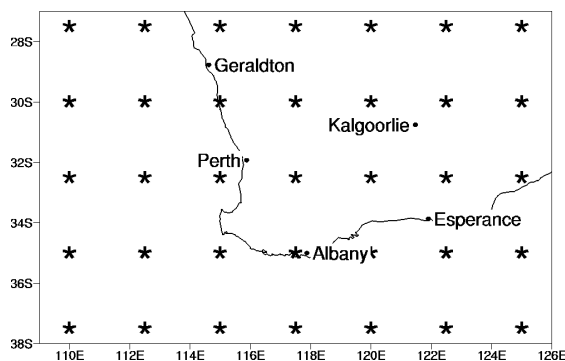

Figure 1.14. 2.5°×2.5° resolution in the southwest region

Pressure
Sea-level pressure is classified in the category with the most influence from observations (Kalnay 1996). The numerical model used for creating the ERA40 data is a more recent model run at higher resolution than that used for the NCEP/NCAR reanalysis, and for many features since 1979 the results are closer to observations. Prior to 1979 the sea-level pressures from ERA40 do not follow the data as closely as does the NCEP/NCAR reanalysis (Figure 1.15). From about 1976 the ERA40 and NCEP/NCAR values are very close.
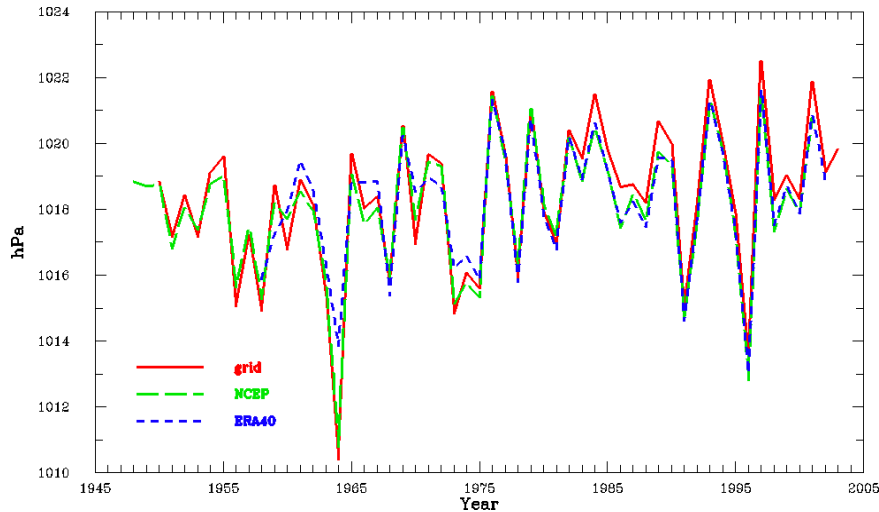
Figure 1.15. June and July average sea-level pressure. Gridded station data averaged over southwest Western Australia, and NCEP/NCAR and ERA40 reanalysis from a point in the southwest.

Rainfall

Precipitation is model-based, and as such is in the least reliable data category (Kalnay 1996). Both NCEP/NCAR and ERA40 provide 'stratiform' and 'convective' rainfall, the sum of which corresponds to the total. Interestingly, the majority of the rainfall over the southwest is from convective rainfall in the NCEP/NCAR reanalysis, and from stratiform rainfall in ERA40; this difference highlights the different parameterisations for precipitation in the reanalyses models. From Figure 1.16 it can be seen that both NCEP/NCAR and ERA40 rainfall output at a point in the southwest vary to a greater extent from data than the sea-level pressure in Figure 1.15. Both reanalyses capture the year to year variability in precipitation at times, though neither reflect the drying trend seen in the station data. The results here indicate that the reanalyses reflect the circulation reasonably accurately, but not the rainfall.
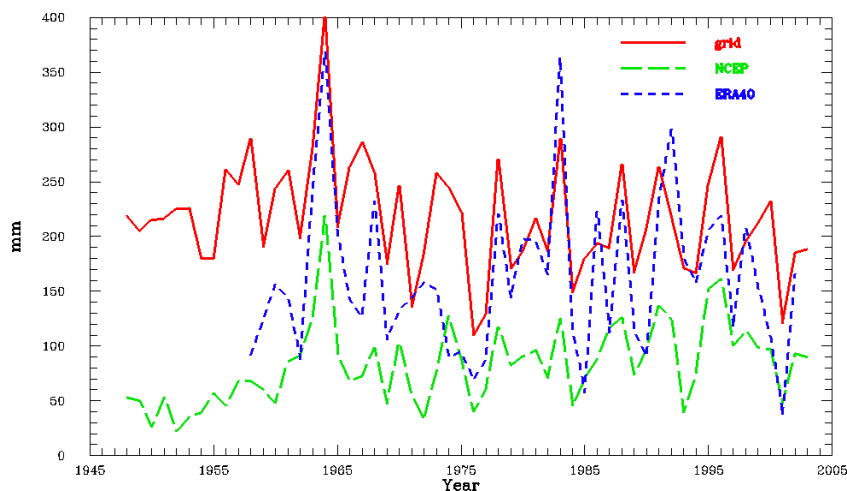

Figure 1.16. June and July precipitation: gridded data averaged over the southwest, and NCEP/NCAR and ERA40 reanalysis from a single point in southwest Western Australia.

20